

1 **The gene *cortex* controls scale colour identity in *Heliconius***

2

3 **Luca Livraghi<sup>1,2</sup>, Joseph J. Hanly<sup>1,2,3</sup>, Ling Sheng Loh<sup>2</sup>, Anna Ren<sup>2</sup>, Ian A. Warren<sup>1</sup>, Carolina**  
4 **Concha<sup>2</sup>, Charlotte Wright<sup>1</sup>, Jonah M. Walker<sup>1</sup>, Jessica Foley<sup>2</sup>, Henry Arenas-Castro<sup>2</sup>, Lucas**  
5 **Rene Brenes<sup>2</sup>, Arnaud Martin<sup>3</sup>, W. Owen McMillan<sup>2</sup> and Chris D. Jiggins<sup>1,2</sup>**

6

7 **Author affiliations:**

- 8 1. Department of Zoology, University of Cambridge, Downing St., Cambridge, CB2 3EJ, UK  
9 2. Smithsonian Tropical Research Institute, Gamboa, Panama  
10 3. The George Washington University Department of Biological Sciences, Science and  
11 Engineering Hall 6000, 800 22<sup>nd</sup> St NW Washington, DC 20052, USA

12

13 **Corresponding author:** Luca Livraghi, University of Cambridge, Cambridge, UK. Dept. of Zoology.  
14 ll566@cam.ac.uk.

15 **Funding:**

16 This work was funded by a grant from the BBSRC to CJ and supported LL (BB/R007500/1); the  
17 National Science Foundation awards IOS-1656553 and IOS-1755329 to AM; a Wellcome Trust PhD  
18 studentship awarded to JJH, a Smithsonian Institution grant to WOM and a Balfour-Browne Trust  
19 studentship to J.M.W.

20 **Keywords:**

21 Evolution, wing patterning, *cortex*, *Heliconius*, cell fate, CRISPR, Lepidoptera.

## 22 **Abstract**

23 The wing patterns of butterflies are an excellent system with which to study phenotypic evolution. The  
24 incredibly diverse patterns are generated from an array of pigmented scales on a largely two-  
25 dimensional surface, resulting in a visibly tractable system for studying the evolution of pigmentation.  
26 In *Heliconius* butterflies, much of this diversity is controlled by a few genes of large effect that regulate  
27 pattern switches between races and species across a large mimetic radiation. One of these genes – *cortex*  
28 - has been repeatedly mapped in association with colour pattern evolution in both *Heliconius* and other  
29 Lepidoptera, but we lack functional data supporting its role in modulating wing patterns. Here we  
30 carried out CRISPR knock-outs in multiple *Heliconius* species and show that *cortex* is a major  
31 determinant of scale cell identity. Mutant wing clones lacking *cortex* showed shifts in colour identity,  
32 with melanic and red scales acquiring a yellow or white state. These homeotic transformations include  
33 changes in both pigmentation and scale ultrastructure, suggesting that *cortex* acts during early stages of  
34 scale cell fate specification rather than during the deployment of effector genes. In addition, mutant  
35 clones were observed across the entire wing surface, contrasting with other known *Heliconius* mimicry  
36 loci that act in specific patterns. Cortex is known as a cell-cycle regulator that modulates mitotic entry  
37 in *Drosophila*, and we found the Cortex protein to accumulate in the nuclei of the polyploid scale  
38 building cells of the butterfly wing epithelium, speculatively suggesting a connection between scale cell  
39 endocycling and colour identity. In summary, and while its molecular mode of action remains  
40 mysterious, we conclude that *cortex* played key roles in the diversification of lepidopteran wing patterns  
41 in part due to its switch-like effects in scale identity across the entire wing surface.

42

## 43 Introduction

44 Evolutionary hotspots have become a recurrent theme in evolutionary biology, whereby variation  
45 surrounding homologous loci at both micro- and macro-evolutionary scales have driven parallel cases  
46 of phenotypic change. Notably, a remarkable 138 genes have been linked to phenotypic variation in 2  
47 or more species (GepheBase; Courtier-Orgogozo et al., 2020). In some cases, parallel adaptation has  
48 occurred through the alteration of downstream effector genes, such as pigmentation enzymes with  
49 functions clearly related to the trait under selection (e.g. *tan*, *ebony*). In other cases, upstream patterning  
50 factors are important, and these are typically either transcription factors (e.g. *optix*, *pitx1*, *Sox10*) or  
51 components of signalling pathways such as ligands or receptors (e.g. *WntA*, MC1R). These classes of  
52 genes influence cell fate decisions during development by modulating downstream gene regulatory  
53 networks (Kronforst and Papa, 2015; Martin and Courtier-Orgogozo, 2017; Prud'homme et al., 2007),  
54 and are commonly characterised by highly conserved functions, with rapid evolutionary change  
55 occurring through regulatory fine-tuning of expression patterns. One gene that has been repeatedly  
56 implicated in morphological evolution but is conspicuous in its failure to conform to this paradigm is  
57 *cortex*, a gene implicated in the regulation of adaptive changes in the wing patterning of butterflies and  
58 moths.

59 *Cortex* is one of four major effect genes that act as switch loci controlling both scale structure and colour  
60 patterns in *Heliconius* butterflies, and has been repeatedly targeted by natural selection to drive  
61 differences in pigmentation (Nadeau, 2016; Van Belleghem et al., 2017). Three of the four major effect  
62 genes correspond to the prevailing paradigm of highly conserved patterning genes; the signalling ligand  
63 *WntA* (Concha et al., 2019; Mazo-Vargas et al., 2017) and two transcription factors *optix* (Lewis et al.,  
64 2019; Zhang et al., 2017) and *aristaless1* (Westerman et al., 2018). The fourth is *cortex*, an insect-  
65 specific gene showing closest homology to the *cdc20/fizzy* family of cell cycle regulators (Chu et al.,  
66 2001; Nadeau et al., 2016; Pesin and Orr-Weaver, 2007). The lepidopteran orthologue of *cortex* displays  
67 rapid sequence evolution, and has acquired novel expression domains that correlate with melanic wing  
68 patterns (Nadeau et al., 2016; Saenko et al., 2019). It therefore seems likely that the role of *cortex* in  
69 regulating wing patterns has involved a major shift in function, which sits in contrast to the classic  
70 model of regulatory co-option of deeply conserved patterning genes, that can be readily applied to other  
71 major *Heliconius* patterning loci.

72 The genetic locus containing *cortex* was originally identified in the genus *Heliconius* as controlling  
73 differences in yellow and white wing patterns in *H. melopmene* and *H. erato* (Figure 1a) and the  
74 polymorphism in yellow, white, black and orange elements in *H. numata*, using a combination of  
75 association mapping and gene expression data (Joron et al., 2006; Nadeau et al., 2016). The same locus  
76 has also been repeatedly implicated in controlling colour pattern variation among divergent  
77 Lepidoptera, including the peppered moth *Biston betularia* and other geometrids, the silkworm *Bombyx*

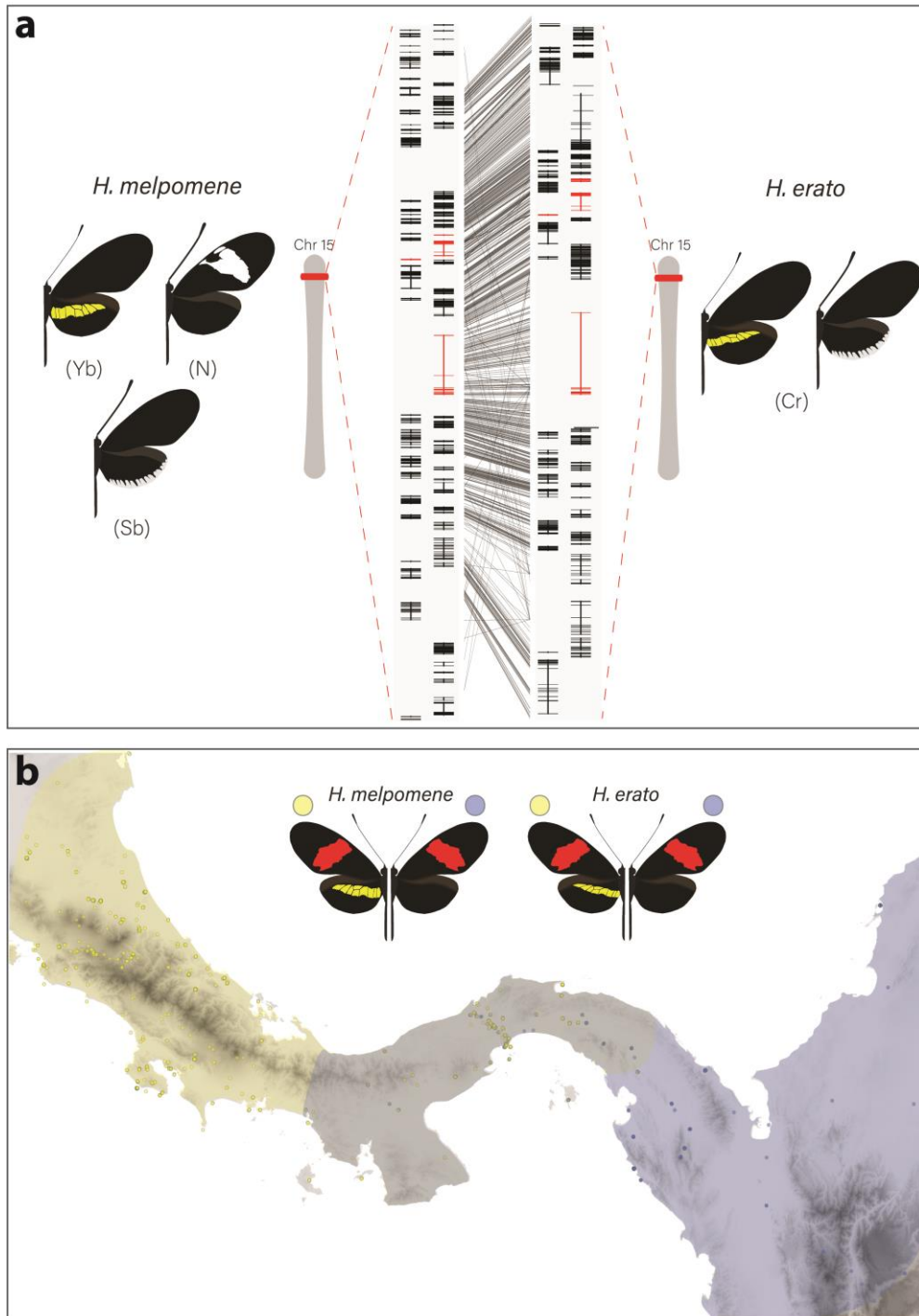
78 *mori* and other butterflies such as *Bicyclus anynana* and *Papilio clytia* (Beldade et al., 2009; Ito et al.,  
79 2016; VanKuren et al., 2019; Van't Hof et al., 2019; Van't Hof et al., 2016). This locus therefore  
80 contains one or more genes that have repeatedly been targeted throughout the evolutionary history of  
81 the Lepidoptera to generate phenotypic diversity.

82 While *cortex* remains the most likely candidate driving yellow and white scale evolution in *Heliconius*,  
83 other genes at the locus may also be playing a role in establishing scale colour identity. Most notably,  
84 the genes *domeless* (*dome*), a JAK-STAT pathway receptor and *washout* (*wash*), a cytoskeleton  
85 regulator, which also show associations with colour pattern phenotypes in *H. melpomene* and *H. numata*  
86 (Nadeau et al., 2016; Saenko et al., 2019). It is thus possible that multiple linked genes are contributing  
87 to the evolution of wing patterning across Lepidoptera (Joron et al., 2006; Saenko et al., 2019).

88 While fantastically diverse, most of the pattern variation in *Heliconius* is created by the differences in  
89 the distribution of only three major scale cell types; Type I (yellow/white), Type II (black), and Type  
90 III (red/orange/brown) (Aymone et al., 2013; Gilbert et al., 1987). Each type has a characteristic  
91 nanostructure and a fixed complement of pigments. Type I yellow scales contain the ommochrome  
92 precursor 3-hydroxykynurenine (3-OHK) (Finkbeiner et al., 2017; Koch, 1993; Reed et al., 2008),  
93 whereas Type I white scales lack pigment, and the colour is the result of the scale cell morphology (i.e.  
94 structural) (Gilbert et al., 1987). In contrast, Type II scale cells are pigmented with melanin and Type  
95 III scale cells contain the red ommochrome pigments xanthommatin and dihydroxanthommatin.

96 Here we focus on the role of *cortex* in *Heliconius* butterflies, an adaptive radiation with over 400  
97 different wing forms in 48 described species (Jiggins, 2017; Lamas, 2004) and where diversity in wing  
98 patterns can be directly linked to the selective forces of predation and sexual selection (Brown, 1981;  
99 Turner, 1981). Specifically, we combine expression profiling using *RNA-seq*, *in situ* hybridization and  
100 antibody staining experiments, as well as CRISPR/Cas9 gene knock-outs to determine the role that this  
101 locus plays in pattern variation of two co-mimetic races of *H. melpomene* and *H. erato* (Figure 1b).

102 Despite the fact that *cortex* does not follow the prevailing paradigm of patterning loci, we demonstrate  
103 for the first time that the gene plays a fundamental role in pattern variation by modulating a switch from  
104 Type I scale cells to Type II and Type III scale cells. Moreover, we show that the phenotypic effects of  
105 *cortex* extend across the fore- and hindwing surface. Our findings, coupled with recent functional  
106 experiments on other *Heliconius* patterning loci, are beginning to illuminate how major patterning genes  
107 interact during development to determine scale cell fate and drive phenotypic variation across a  
108 remarkable adaptive radiation.



109

**Figure 1 – Ranges of *Heliconius* butterflies differing at Yb phenotypes in Central America and associated loci**

(a) Homologous loci in both species are associated with variation in yellow and white patterns between races. In *H. melpomene* three tightly linked genetic elements located at chromosome 15 control variation for hindwing yellow bar, forewing band and white margin elements (Yb, N and Sb respectively) while in *H. erato* variation has been mapped to one element (Cr). Genes previously associated with wing patterning differences in Lepidoptera are highlighted in red within a specific region of chromosome 15 (from bottom up; *cortex*, *domeless-truncated*, *domeless* and *washout*) and alignment between the two co-mimetic species at the locus is shown (grey lines, 95% alignment identity). (b) Focal co-mimetic races of *Heliconius erato* and *Heliconius melpomene* used in this study, differing for the presence of a hindwing yellow bar, and their ranges across Central America are shown (ranges based on Rosser et al., 2012). Yellow: yellow banded races, blue: black hindwing races, grey: range overlap.

## 110 Results

### 111 *RNA-seq* and reannotation of key intervals reveals the presence of duplications and bi-cistronic 112 transcription of candidate genes

113 In order to identify genes associated with differences in yellow pattern elements, we performed  
114 differential gene expression (DGE) analysis using developing wings sampled from colour pattern races  
115 in *H. erato* and *H. melpomene* differing only in the presence or absence of the hindwing yellow bar  
116 (Figure 1b and Figure 2a). In total, we sequenced 18 samples representing three developmental stages  
117 (larval, 36h +/-1.5h (Day 1 pupae) and 60h +/- 1.5h (Day 2 pupae)) from two races in each of the two  
118 species, with hindwings divided into two parts for the pupal stages (Figure 2a). We focused our attention  
119 on genes centred on a 47-gene interval on chromosome 15 previously identified as the minimal  
120 associated region with yellow band phenotypes by recombination mapping (Nadeau et al., 2016, supp  
121 table 1; Joron et al., 2006; Moest et al., 2020; Van Belleghem et al., 2017). Both our initial expression  
122 analysis and recent analysis of selective sweeps at this locus (Moest et al., 2020) indicate that three  
123 genes showed differential expression and are likely targets of selection: *cortex*, *dome* and *wash* (Figure  
124 2c). This led us to further explore the annotation of these genes prior to further analysis.

125 In *Heliconius*, *dome* appears to have duplicated in the ancestor of *H. erato* and *H. melpomene*, resulting  
126 in a full-length copy (referred to here as *domeless*) and a further copy exhibiting truncations at the C-  
127 terminus (*domeless-truncated*) (Supplementary File 1 – Figure S1). Independent tandem duplications  
128 of *dome* have occurred in several other Lepidoptera. Protein alignments indicate that in both *H. erato*  
129 and *H. melpomene*, *dome-trunc* maintains only the N-terminal half of the gene, suggesting *dome-trunc*  
130 is undergoing pseudogenisation.

131 When examining the *RNA-seq* reads mapping to the *dome* and *wash* genes, we observed several  
132 individual reads splicing over the 5' UTR of *wash* and into the coding region of *dome*. It was not  
133 possible to unambiguously assign reads that map to this overlapping portion of the annotation to either  
134 gene, suggesting the possibility that *dome/wash* are transcribed as a single, bi-cistronic transcript. To  
135 look for further evidence of co-transcription, we searched the Transcription Shotgun Assembly (TSA)  
136 sequence archive on NCBI for assembled transcripts containing the open reading frames (ORFs) of both  
137 genes in other Lepidoptera (Supplementary File 2 – Figure S2). We found several instances where ORFs  
138 encoding for both *dome* and *wash* can be found in a single transcript, suggesting bi-cistronic  
139 transcription is a conserved feature across butterflies. Furthermore, an examination of published *ATAC-*  
140 *seq* peaks (Lewis et al., 2019), shows the presence of a single promoter at the start of *dome* for *H. erato*  
141 *lativitta*, suggesting both genes share a single transcription start site (Supplementary File 2 – Figure  
142 S2). Given this result, we repeated the DGE analysis with *dome/wash* as a single annotation.

143 **The genes *cortex* and *domeless/washout* are differentially expressed between colour pattern races,**  
144 **and between wing sections differing in the presence of the hindwing yellow bar**

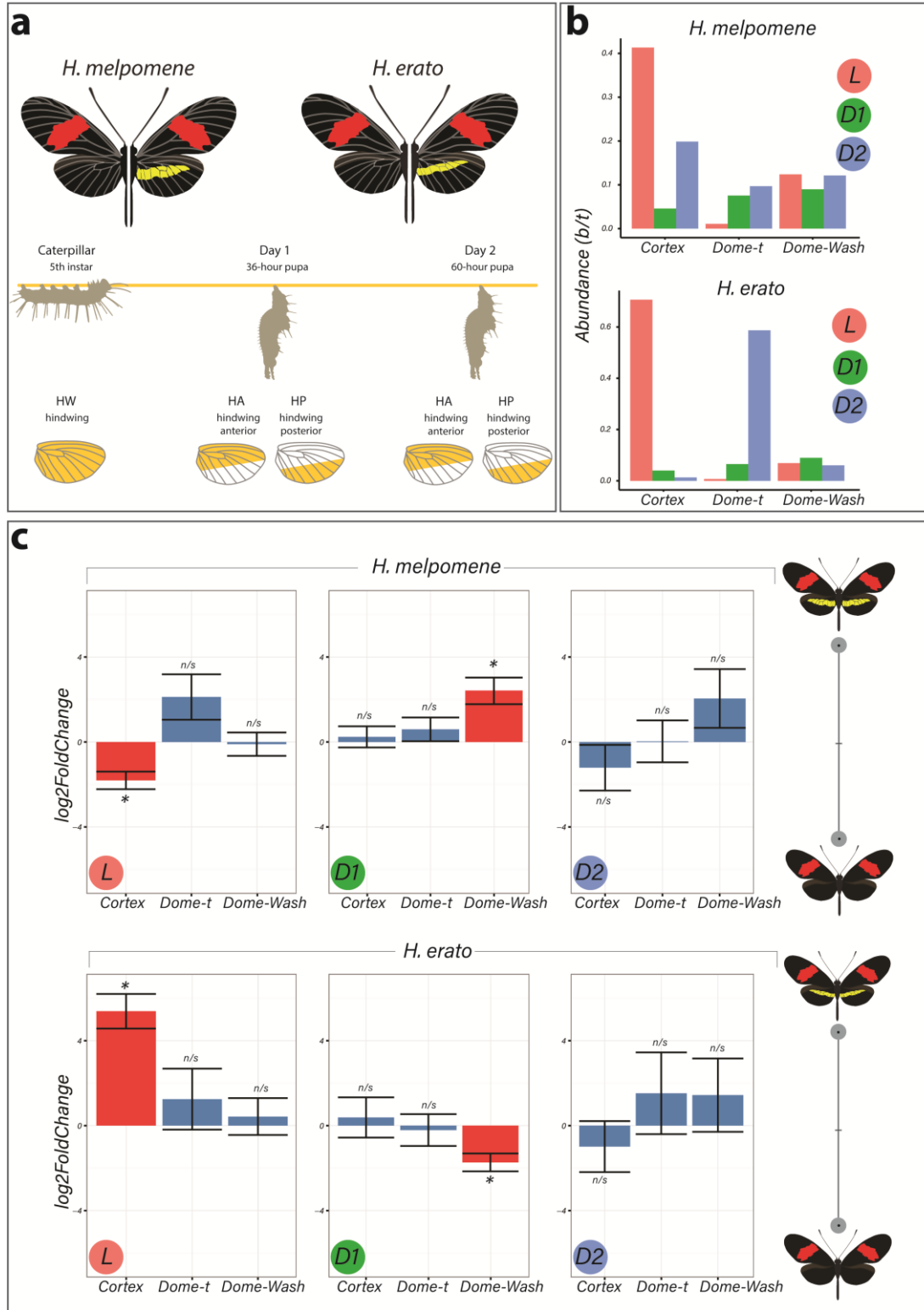
145 *RNA-seq* data show *cortex* transcripts were most abundant in 5<sup>th</sup> instar larvae, almost depleted in Day 1  
146 pupae, but were again detected at relatively high levels in Day 2 pupae in *H. melpomene*, suggesting  
147 dynamic expression in this species (Figure 2b). In *H. erato*, *cortex* transcripts are found in high  
148 abundance in 5<sup>th</sup> instar larvae but are almost depleted in Day 1 and Day 2 pupae. Both *dome* paralogs  
149 remain relatively constant in terms of expression across all stages in *H. melpomene* whereas *dome-trunc*  
150 expression increases in pupal stages in *H. erato*. *Dome/wash* transcripts are detected in relatively low  
151 and constant amounts in both species.

152 The two species were analysed separately, with both showing only *cortex* and *dome/wash* as  
153 significantly differentially expressed between morphs among the 47 genes in the candidate region, with  
154 *cortex* differential expression occurring earlier in development. In fifth instar larvae, *cortex* is  
155 differentially expressed in both species between the two colour pattern races, with *cortex* showing the  
156 highest adjusted *p*-value for any gene in the genome at this stage in *H. erato* (Figure 2c). Interestingly,  
157 *cortex* transcripts were differentially expressed in opposite directions in the two species, with higher  
158 expression in the melanic hindwing race in *H. melpomene*, and in the yellow banded race in *H. erato*.  
159 This pattern is reversed for *dome/wash* in Day 1 pupae, where a statistically higher proportion of  
160 transcripts are detected in *H. melpomene rosina* (yellow), and in *H. erato hydara* (melanic). No  
161 differential expression of these genes was found at Day 2 pupae. In order to confirm this inverted pattern  
162 was not due to a sampling error, we performed a diagnostic SNP analysis by correlating coding SNPs  
163 found within protein coding genes at the *cortex* locus from whole genome sequence data to the  
164 corresponding *RNA-seq* datasets (Supplementary File 3 – Tables S3.1 and S3.2).

165 When comparing across hindwing sections differing for the yellow bar phenotype, 22 genes out of the  
166 associated 47-gene interval were differentially expressed at Day 1 between relevant wing sections in *H.*  
167 *melpomene*, including *cortex* and *dome/wash* (Supplementary File 4 – Figures S4.1 and S4.2). In  
168 contrast in *H. erato* Day 1 pupae, only *dome/wash* was differentially expressed. At Day 2 pupae, there  
169 were no differentially expressed genes in either species between relevant wing sections at this locus.

170 Given the strong support for the involvement of *cortex* in driving wing patterning differences, we re-  
171 analysed its phylogenetic relationship to other *cdc20* family genes with more extensive sampling than  
172 previous analyses (Nadeau et al., 2016). Our analysis finds strong monophyletic support for *cortex* as  
173 an insect-specific member of the *cdc20* family, with no clear *cortex* homologs found outside of the  
174 Neoptera (Supplementary File 5 – Figure S5.1). Branch lengths indicate *cortex* is evolving rapidly  
175 within the lineage, despite displaying conserved APC/C binding motifs, including the C-Box and IR  
176 tail (Supplementary File 5 – Figure S5.2) (Chu et al., 2001; Pesin and Orr-Weaver, 2007).

177 In summary, *cortex* is the most consistently differentially expressed gene and showed differential  
 178 expression earlier in development as compared to the other candidate *dome/wash*. We therefore focus  
 179 subsequent experiments on *cortex*, although at this stage we cannot rule out an additional role for  
 180 *dome/wash* in pattern specification.



181



**Figure 2 – Differential expression of genes at Chromosome 15 implicate *cortex* as most likely candidate driving yellow bar differences**

(a) Hindwing tissue from co-mimetic races of *H. melpomene* and *H. erato* were collected at three developmental stages (5<sup>th</sup> instar caterpillar, Day 1 Pupae (36hAPF) and Day 2 Pupae (60hAPF)). For pupal tissue, hindwing tissue was dissected using the wing vein landmarks shown, corresponding to the future adult position of the hindwing yellow bar (dissection scheme based on Hanly et al., 2019). (b) Relative abundance of transcripts corresponding to the genes *cortex*, *domeless-truncated*, *domeless/washout* throughout developmental stages. *Cortex* expression decreases from larval to pupal stages *domeless-truncated* expression increases, whereas *domeless/washout* stay relatively constant at all three stages. (c) Log<sub>2</sub>FoldChange for the genes *cortex*, *domeless-truncated*, *domeless/washout* across developmental stages. Comparisons are for whole wing discs (Larvae, L) and for contrast C for pupae (D1 and D2; see Supplementary File 4: Figure S4.3 for depiction of contrasts analysed).

182

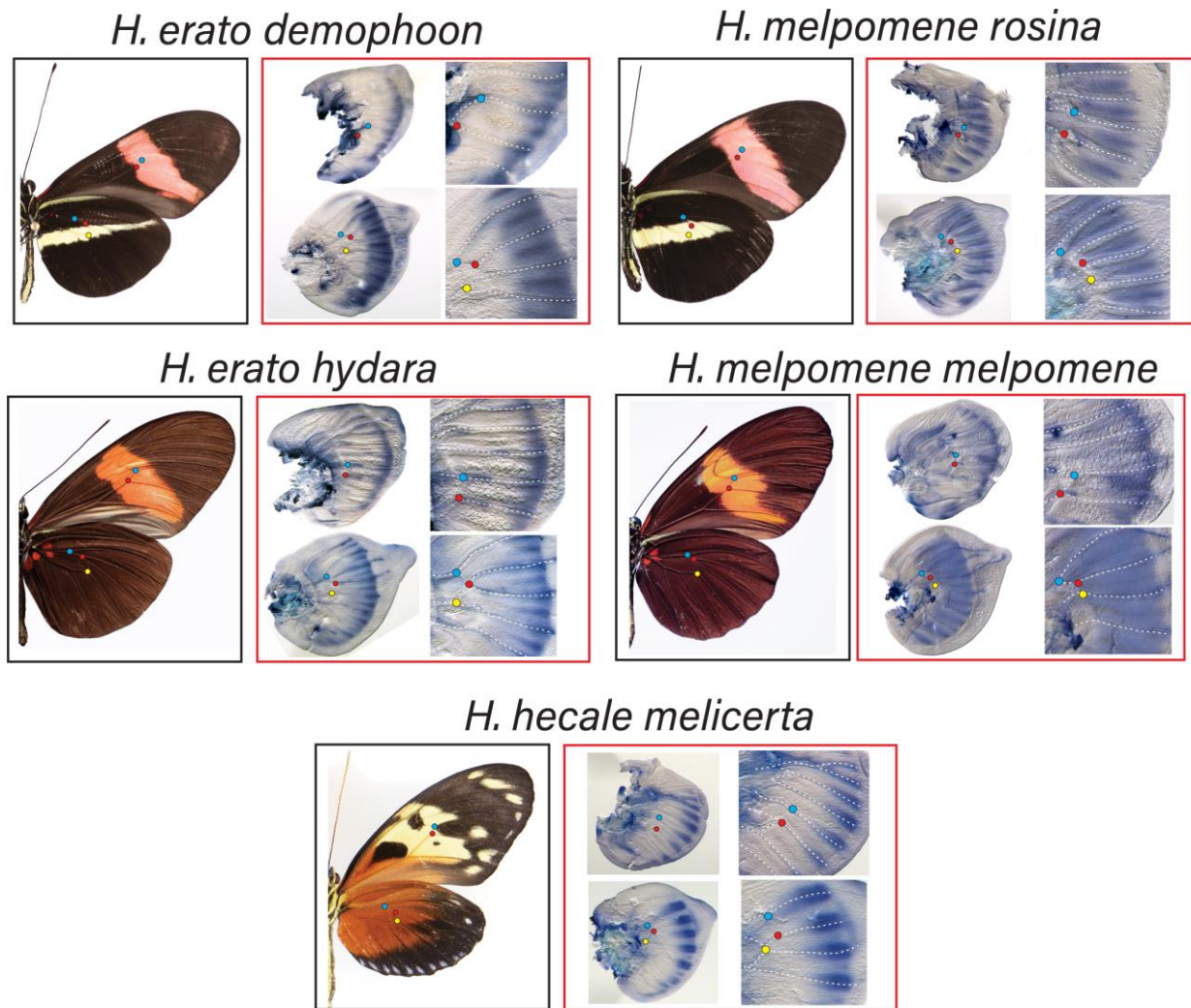
183 ***Cortex* transcripts localise distally in 5<sup>th</sup> instar larvae**

184 Two studies have reported that *cortex* mRNA expression correlates with melanic patch in two species  
185 of *Heliconius* (Nadeau et al., 2016 and Saenko et al., 2019). To further assess this relationship between  
186 *cortex* expression and adult wing patterns, we performed *in situ* hybridisation on developing wing discs  
187 of 5<sup>th</sup> instar larvae, where we observed largest *cortex* transcript abundance, in both the yellow-barred  
188 and plain hindwing morphs of *H. erato* and *H. melpomene*. *Cortex* transcripts at this stage localised  
189 distally in forewings and hindwings of both species (Figure 3). In *H. erato demophoon*, expression was  
190 strongest at the intervein midline, but extends across vein compartments covering the distal portion of  
191 both forewing and hindwing. By contrast, in *H. erato hydara*, *cortex* transcripts are more strongly  
192 localised to the intervein midline forming a distally localised intervein expression domain.

193 Expression in *H. melpomene rosina* is similar to *H. erato demophoon* at comparable developmental  
194 stages, again with stronger expression localised to the intervein midline but extending further  
195 proximally than in *H. erato demophoon*. In *H. melpomene melpomene*, hindwing *cortex* expression  
196 extends across most of the hindwing, and does not appear to be restricted to the intervein midline.

197 Given that *cortex* has been implicated in modulating wing patterns in many divergent lepidoptera, we  
198 examined localisation in a *Heliconius* species displaying distinct patterns: *H. hecale melicerta* (Figure  
199 3). Interestingly, in this species transcripts appear strongest in regions straddling the wing disc veins,  
200 with weak intervein expression observed only in the hindwings. Previous data has shown variation in  
201 yellow spots (Hspot) is also controlled by a locus located a chromosome 15 (Huber et al., 2015).  
202 Expression in *H. hecale melicerta* forewings corresponds to melanic regions located in between yellow  
203 spots at the wing margins, indicating *cortex* may be modulating Hspot variation in *H. hecale*.

204 Overall, our results suggest a less clear correlation to melanic elements than reported expression  
205 patterns (Nadeau et al., 2016; Saenko et al., 2019) where *cortex* expression in 5<sup>th</sup> instar caterpillars is  
206 mostly restricted to the distal regions of developing wings, but appears likely to be dynamic across 5<sup>th</sup>  
207 instar development.



208

**Figure 3 – Expression of *cortex* transcripts in *H. melpomene*, *H. erato* and *H. hecale* 5<sup>th</sup> instar wing discs**

*Cortex* expression in 5<sup>th</sup> instar wing discs is restricted to the distal end of both forewings and hindwings in all species and morphs analysed. In *H. erato*, expression is strongest at the intervein midline but extends across vein compartments in *H. erato demophoon*, whereas it is more strongly localised to the intervein midline in *H. erato hydrara*. In *H. melpomene rosina*, *cortex* localises in a similar manner to *H. erato demophoon*, with stronger expression again observed at the intervein midline, whereas expression in *H. melpomene melpomene* extends more proximally. Coloured dots represent homologous vein landmarks across the wings.

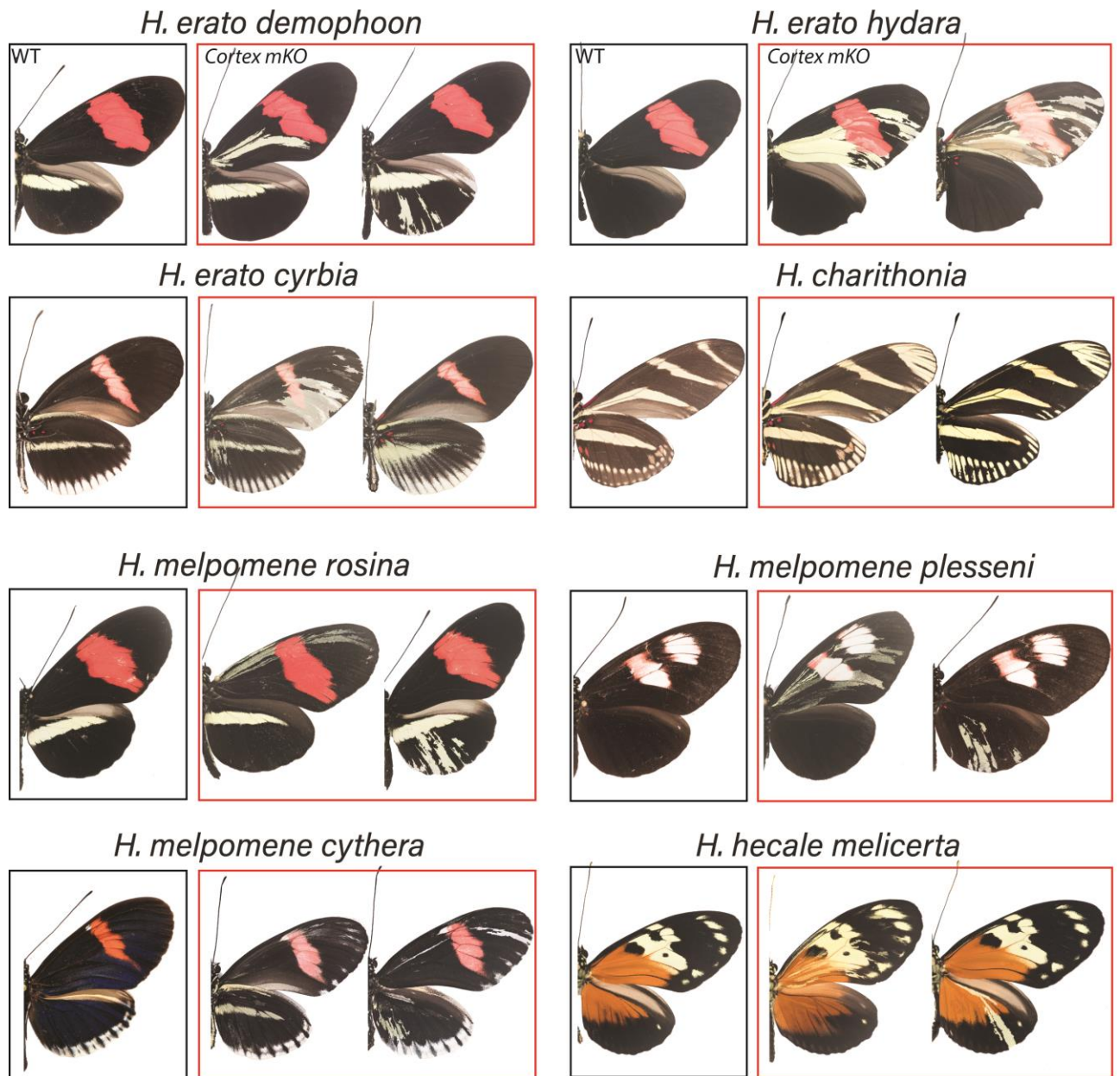
209 ***Cortex* establishes Type II and III scale identity in *Heliconius* butterflies**

210 To assay the function of *cortex* during wing development, we used CRISPR/Cas9 to generate G<sub>0</sub>  
211 somatic mosaic mutants (crispants) (Mazo-Vargas et al., 2017; Zhang et al., 2017). We targeted  
212 multiple exons using a combination of different guides and genotyped the resulting mutants through  
213 PCR amplification, cloning and Sanger sequencing (Supplementary File 6 – Figure S6). Overall KO  
214 efficiency was low when compared to similar studies in *Heliconius* (Concha et al., 2019; Mazo-Vargas  
215 et al., 2017), with observed wing phenotype to hatched eggs ratios ranging from 0.3% to 4.8%. Lethality

216 was also high, with hatched to adult ratios ranging from 8.1% to 29.8% (Supplementary File 7 – Table  
217 S7.1).

218 Targeting of the *cortex* gene in *H. erato* produced patches of ectopic yellow and white scales spanning  
219 regions across both forewings and hindwings (Figure 4 and Supplementary File 8 – Figures S8.1-S8.7).  
220 Both colour pattern races were affected in a similar manner in *H. erato*. Mutant clones were not  
221 restricted to any specific wing region, affecting scales in both proximal and distal portions of wings.  
222 The same effect on scale pigmentation was also observed in the co-mimetic morphs in *H. melpomene*,  
223 with mutant clones affecting both distal and proximal regions in forewings and hindwings. In *H. erato*  
224 *hydara*, we recovered a mutant individual where clones spanned the dorsal forewing band. Clones  
225 affecting this region caused what appears to be an asymmetric deposition of pigment across the scales,  
226 as well as transformation to white, unpigmented scales (Figure 5 and Supplementary File 9 – Figure  
227 S9).

228 As this locus has been associated with differences in white hindwing margin phenotypes (Jiggins and  
229 McMillan, 1997) (Figure 1b), we also targeted *cortex* in mimetic races showing this phenotype, *H. erato*  
230 *cyrbia* and *H. melpomene cythera*. Mutant scales in these colour pattern races were also localised across  
231 both wing surfaces, with both white and yellow ectopic scales. In these races, a positional effect was  
232 observed, where ectopic scales in the forewing and anterior compartment of the hindwing shifted to  
233 yellow, and posterior hindwing scales became white (Figure 4 and Supplementary File 9 – Figure S9).  
234 This positional effect likely reflects differential uptake of the yellow pigment 3-OHK across the wing  
235 surface (Reed et al., 2008). For one individual of *H. erato cyrbia*, clones also extended across the red  
236 band where a shift to white scales was observed, as in *H. erato hydara*.



237

**Figure 4 – *Cortex* loss of function transforms scale identity across the entire wing surface**

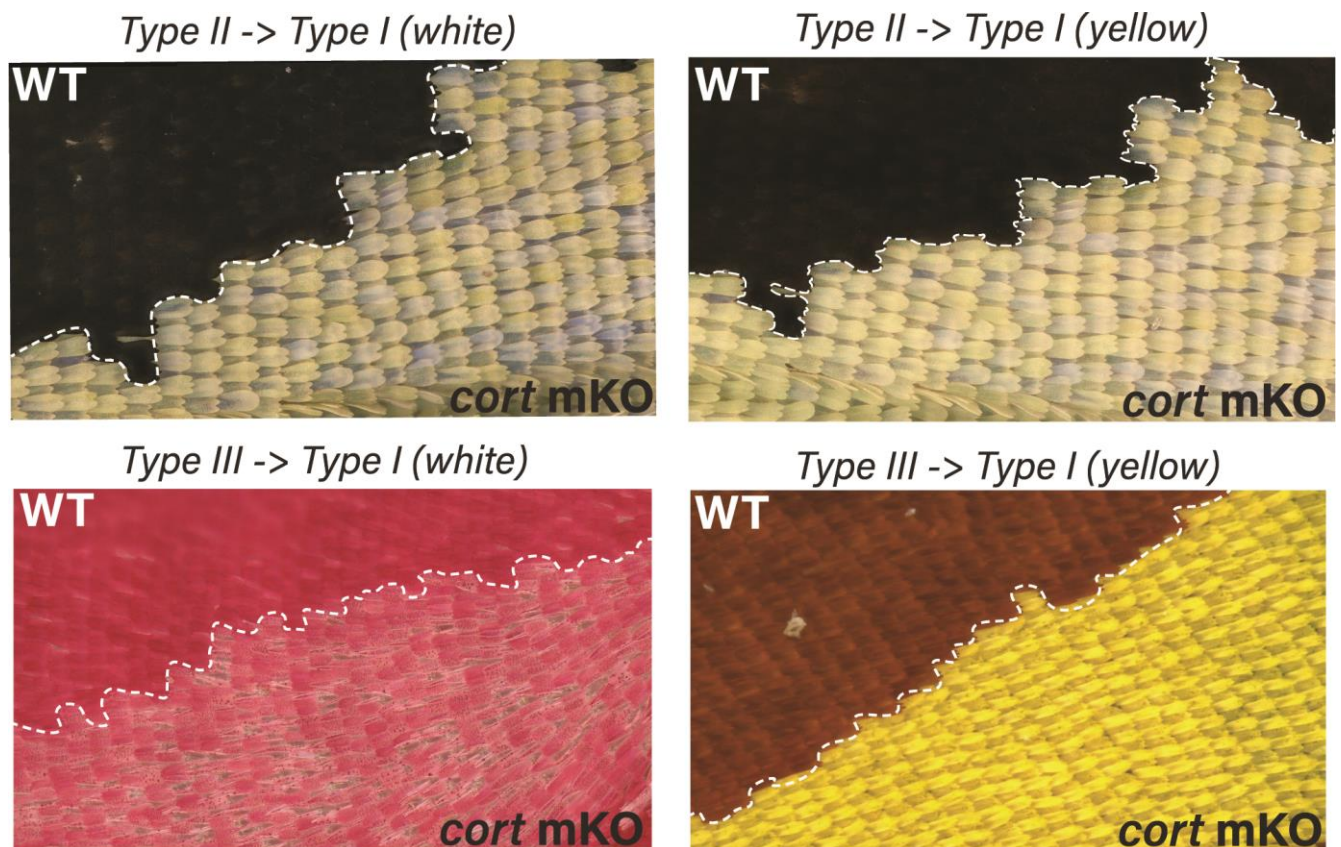
Phenotypes of *cortex* mKO across *Heliconius* species and morphs reveals a loss of melanic (Type II) and red (Type III) scales, and transformation to Type I (yellow or white) scales. Affected regions are not spatially restricted, and span both distal and proximal portions of forewings and hindwings. A positional effect is observed in some races, where ectopic Type I scales are either white or yellow depending on their position along the wing (e.g. *H. erato cyrbia*). Ectopic Type I scales can be induced from both melanic and red scales, switching to either white or yellow depending on wing position and race. Boundaries between Wild-type (WT) to mutant scales are highlighted (dotted white line).

238 To further test the conservation of *cortex* function across the *Heliconius* radiation, we knocked out  
239 *cortex* in *H. charithonia* and *H. hecale melicerta*, outgroups to *H. erato* and *H. melpomene* respectively.  
240 Again, ectopic yellow and white scales appeared throughout the wing surface in both species,  
241 suggesting conserved function with respect to scale development among *Heliconius* butterflies. In *H.*

242 *hecale melicerta*, we also recovered a mutant where we saw transformation from orange ommochrome  
243 scales to yellow.

244 In summary, *cortex* crispants appear to not be restricted to any specific wing pattern elements, and  
245 instead affect regions across the surface of both forewings and hindwings. Mutant scales are always  
246 Type I scales, with differing pigmentation (3-OHK, yellow) or structural colouration (white) depending  
247 on race and wing position (Figure 5). The high rate of mosaicism combined with high mortality rates  
248 suggests *cortex* is likely developmentally lethal. Furthermore, the sharp boundaries observed between  
249 wild-type and mutant scales suggest *cortex* functions in a cell-autonomous manner, with little or no  
250 communication between neighbouring cells (Figure 5 and Supplementary File 9 - Figure S9).

251



252

253

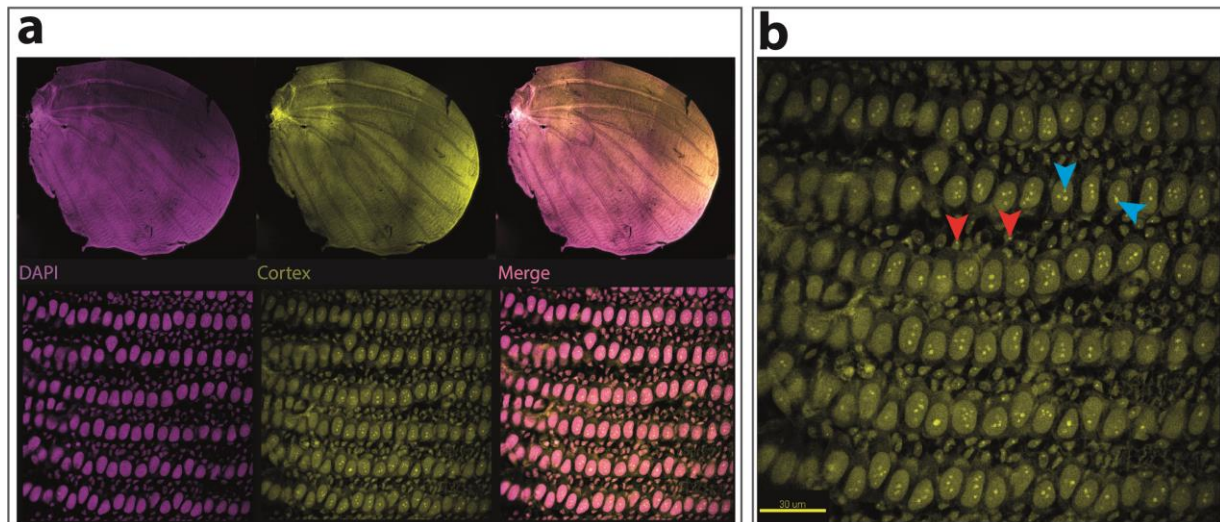
### Figure 5 – CRISPR KOs induce Type I scale identity

Ectopic Type I scales can be induced from both melanic and red scales, switching to either white or yellow depending on wing position and race. Boundaries between Wild-type (WT) to mutant scales are highlighted (dotted white line).

254 **Nuclear localization of Cortex extends across the wing surface in pupal wings**

255 The *cortex* mRNA expression patterns in larval imaginal disks suggest a dynamic progression in the  
256 distal regions, and in a few cases (Figure 3; Nadeau et al., 2016; Saenko et al., 2019) a correlation with  
257 melanic patterns whose polymorphisms associate with genetic variation at the Cortex locus itself. We  
258 thus long hypothesized that like for the *WntA* mimicry gene (Martin et al., 2012, Mazo-Vargas 2017 et  
259 al., Concha et al., 2020), the larval expression domains of *cortex* would delimit the wing territories  
260 where it is playing an active role in colour patterning. However, our CRISPR based loss-of-function  
261 experiments challenge that hypothesis because in all the morphs that we assayed, we found mutant  
262 scales across the wing surface (Figure 6 and supplementary File 9 – Figure S9).

263 This led us to re-examine our model and consider that post-larval stages of Cortex expression could  
264 reconcile the observation of scale phenotypes across the entire wing, rather than in limited areas of the  
265 wing patterns. To test this hypothesis, we developed a Cortex polyclonal antibody, and found nuclear  
266 expression across the epithelium of *H. erato demophoon* pupal hindwings without restriction to specific  
267 pattern element (Figure 6). This nuclear localization overlapped with DNA, also included a strong signal  
268 in the large nucleoli of both the polyploid scale building cells, and their adjacent, non-polyploid  
269 epithelial cells (Greenstein, 1972). Following previous reports suggesting a correlation between  
270 pigmentation state and ploidy level (Cho and Nijhout, 2013; Henke and Pohley, 1952; Iwata and Otaki,  
271 2016), we tested if nuclear volume or nucleoli number would associate with the yellow band, but failed  
272 to find a consistent pattern in the distribution of Cortex protein (Figure 6 and Supplementary File 10 -  
273 Figure S10). However, currently we cannot rule an association of Cortex protein with colour pattern  
274 elements at other developmental stages, and given the apparent dynamic nature of *cortex* expression, a  
275 more precise developmental time series will be required to make more conclusive statements.



276

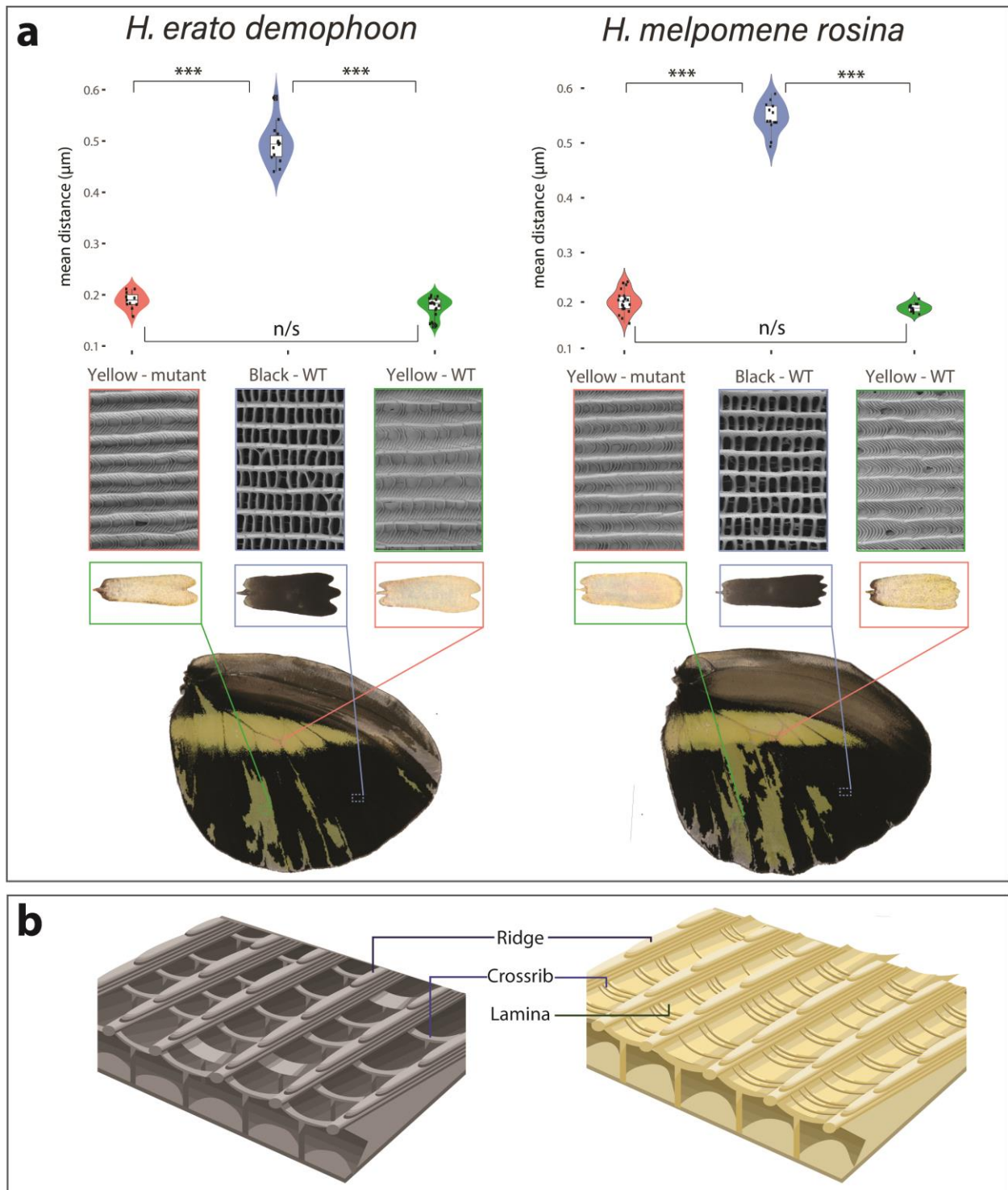
**Figure 6 – Cortex protein localises throughout pupal hindwings in *H. erato demophoon***

(a) Cortex immunostaining reveals presence of Cortex across the hindwing of *H. erato demophoon*. DAPI (left) Cortex (middle) and merged channels (right) are shown. (b) Cortex localises as puncta in the developing pupal cells. Multiple puncta per cell are visible in the large polyploid nuclei (blue arrows) while single puncta localise to the uninuclear epithelium below (red arrows). Scale bar = 30µm.

277 ***Cortex* KO causes homeotic shifts in scale structure.**

278 Previous studies have shown an association between scale ultrastructure and pigmentation in *Heliconius*  
279 butterflies (Concha et al., 2019; Gilbert et al., 1987; Zhang et al., 2017). With this in mind, we tested  
280 whether ectopic yellow/white scales were accompanied by structural homeosis using Scanning Electron  
281 Microscopy. To account for known positional effects on scale structure we compared wild-type and  
282 mutant scales from homologous locations across the wing surface.

283 Ultrastructural differences are consistent with homeosis in *cortex* mutant scales in both *H. melpomene*  
284 and *H. erato* (Figure 7). Cross-rib distance is the same between yellow wild-type and *cortex* mutant  
285 scales, and significantly different between distally located wild-type black scales. A similar relationship  
286 was observed for scale length in both species, but inter-ridge distance and scale width was consistent  
287 with homeosis only in *H. melpomene* (Supplementary File 11 – Figure S11). A consistent difference  
288 between all Type I scales (mutant and wild-type) is the presence of a lamina covering the inter-ridge  
289 space (Figure 7b), suggesting this structure is an important morphological feature of yellow/white scales  
290 (Matsuoka and Monteiro, 2018), and that *cortex* is necessary for the differentiation of lamellar tissue in  
291 *Heliconius* scales.



292

**Figure 7 – SEM reveals structural homeosis is induced in *cortex* KO scales.**

Structural homeosis is induced in *cortex* KO scales in both *H. melpomene* and *H. erato*. Mutant and wild-type scale comparisons from homologous wing positions are shown, illustrating clear ultrastructural homeosis between wild-type and KO yellow scales. Mean cross-rib distance between wild-type and mutant yellow scales is not significantly different, while significantly different between both wild-type yellow and mutant yellow with wild-type black scales (Wilcoxon test, \*\*\* indicates  $p < 0.001$ ).

293



## 294 **Discussion:**

### 295 ***Cortex* is a key scale cell specification gene**

296 The genetic locus containing the gene *cortex* represents a remarkable case of parallel evolution, where  
297 repeated and independent mutations surrounding the gene are associated with shifts in scale  
298 pigmentation state in at least 8 divergent species of Lepidoptera (Beldade et al., 2009; Nadeau et al.,  
299 2016; Van Belleghem et al., 2017; VanKuren et al., 2019; van't Hof et al., 2019; Van't Hof et al., 2016).  
300 While these studies have linked putative regulatory variation around *cortex* to the evolution of wing  
301 patterns, its precise effect on scale cell identity and pigmentation has remained speculative until now.  
302 Here, we demonstrate that *cortex* is a causative gene that specifies melanic and red (Type II and Type  
303 III) scale cell identity in *Heliconius*, and acts by influencing both downstream pigmentation pathways  
304 and scale cell ultrastructure. Moreover, our combination of expression studies and functional knock-  
305 outs demonstrate that this gene acts as a key early scale cell specification switch across the wing surface  
306 of *Heliconius* butterflies, and thus has the potential to generate much broader pattern variation than  
307 previously described patterning genes.

308 While we have shown that *cortex* is a key scale cell specification gene, it remains unclear how a gene  
309 with homology to the fizzy/cdc20 family of cell cycle regulators acts to modulate scale identity. In  
310 *Drosophila*, Fizzy proteins are known to regulate APC/C activity through the degradation of cyclins,  
311 leading to the arrest of mitosis (Raff et al., 2002). In particular, *fizzy-related* (*fzr*), induces a switch from  
312 the mitotic cycle to the endocycle, allowing the development of polyploid follicle cells in *Drosophila*  
313 ovaries (Schaeffer et al., 2004; Shcherbata, 2004). Similarly *cortex* has been shown to downregulate  
314 cyclins during *Drosophila* female meiosis, through its interaction with the APC/C (Pesin and Orr-  
315 Weaver, 2007; Swan and Schüpbach, 2007). Cortex Immunostainings show that Cortex protein  
316 localises to the nucleus in *Heliconius* pupal wings, suggesting a possible interaction with the APC/C in  
317 butterfly scale building cells. Ploidy levels in Lepidoptera scale cells have been shown to correlate with  
318 pigmentation state, where increased ploidy and scale size lead to darker scales (Cho and Nijhout, 2013;  
319 Iwata and Otaki, 2016). *cortex* may thus be modulating ploidy levels by inducing endoreplication cycles  
320 in developing scale cells. However, we currently have no direct evidence for a causal relationship  
321 between ploidy state and pigmentation output, and a mechanistic understanding of this relationship and  
322 any role *cortex* may be playing in modulating ploidy levels will require future investigation.

### 323 ***Heliconius* wing patterning is controlled by interactions among major patterning genes**

324 Functional knockouts now exist for all the 4 major loci known to drive pigmentation differences in  
325 *Heliconius* (Mazo-Vargas et al., 2017; Westerman et al., 2018; Zhang et al., 2017). These loci represent  
326 the major switching points in the GRNs that are ultimately responsible for determining scales cell  
327 identity. This work underscores the importance of two patterning loci, *cortex* and *WntA*, as master

328 regulators of scale cell identity. Both are upregulated early in wing development and have broad effects  
329 on pattern variation (Concha et al., 2019; Nadeau et al., 2016). The signalling molecule *WntA* modulates  
330 forewing band shape in *Heliconius* by delineating boundaries around patterns elements, and is expressed  
331 in close association with future pattern elements (Concha et al., 2019; Martin et al., 2012). Unlike *cortex*  
332 mutants, *WntA* KOs shift scale cell identity to all three cell Types (I, II and III), depending on genetic  
333 background. Thus, *WntA* acts as a spatial patterning signal inducing or inhibiting colour in specific wing  
334 elements, in contrast to *cortex*, which acts as an “on-off” switch across all scales on the butterfly wing.  
335 Interestingly, *cortex* knockouts lead to shifts in scale fate irrespective of *WntA* expression. This suggests  
336 either that *cortex* is required as an inductive signal to allow *WntA* to signal further melanisation, or that  
337 two, independent ways to melanise a scale are available to the developing wing. The latter hypothesis  
338 is supported by certain *H. erato* colour pattern *WntA* mutants, where even in putatively *cortex* positive  
339 regions, scales are able to shift to Type I in the absence of *WntA* alone (Concha et al., 2019). This  
340 suggests that while under certain conditions *cortex* is sufficient to induce the development of black  
341 scales, *WntA* is also required as a further signal for melanisation in some genetic backgrounds. Under  
342 this scenario, colour pattern morphs may be responding epistatically to different *WntA/cortex* alleles  
343 present in their respective genetic backgrounds.

344 Under a simple model (Figure 8), *cortex* is one of the earliest regulators and sets scale differentiation to  
345 a specific pathway switches between Type I (yellow/white) and Type II/III (black/red) scales. Thus, we  
346 can envision a differentiating presumptive scale cell (PSC) receiving a Cortex input as becoming Type  
347 II/III competent, with complete Type III differentiation occurring in the presence of *optix* expression  
348 (Zhang et al., 2017). This is consistent with our data, which shows *cortex* is also required as a signal  
349 for Type III (red) scales to properly develop. Several *cortex* mutant individuals had clones across red  
350 pattern elements, and failed to properly develop red pigment. The development of red scales in  
351 *Heliconius* butterflies is also dependent on expression of the transcription factor *optix* during mid-pupal  
352 development (Lewis et al., 2019; Reed et al., 2011; Zhang et al., 2017). Therefore, *cortex* expression is  
353 required for either downstream signalling to *optix*, or to induce a permissive scale morphology for the  
354 synthesis and deposition of red pigment in future scales. *Cortex* is thus necessary for the induction of  
355 Type III scale cells but insufficient for their proper development.

356 Conversely, a PSC lacking a Cortex input differentiates into a Type I scale, whose pigmentation state  
357 depends on the presence of the transcription factor *aristaless1* (*all*), where *all* is responsible for  
358 inducing a switch from yellow to white scales in *Heliconius* by affecting the deposition of the yellow  
359 pigment 3-OHK (Westerman et al., 2018). The uptake of 3-OHK from the haemolymph occurs very  
360 late in wing development, right before the adult ecloses (Reed et al., 2008). Our *cortex* crispants  
361 revealed a shift to both yellow and white scales, with their appearance being positionally dependent;  
362 more distally located scales generally switch to white, while more proximal scales become yellow

363 (Supplementary File 8 and 9). This pigmentation state is likely controlled by differences in *all*  
 364 expression varying between wing sections in different ways across races.

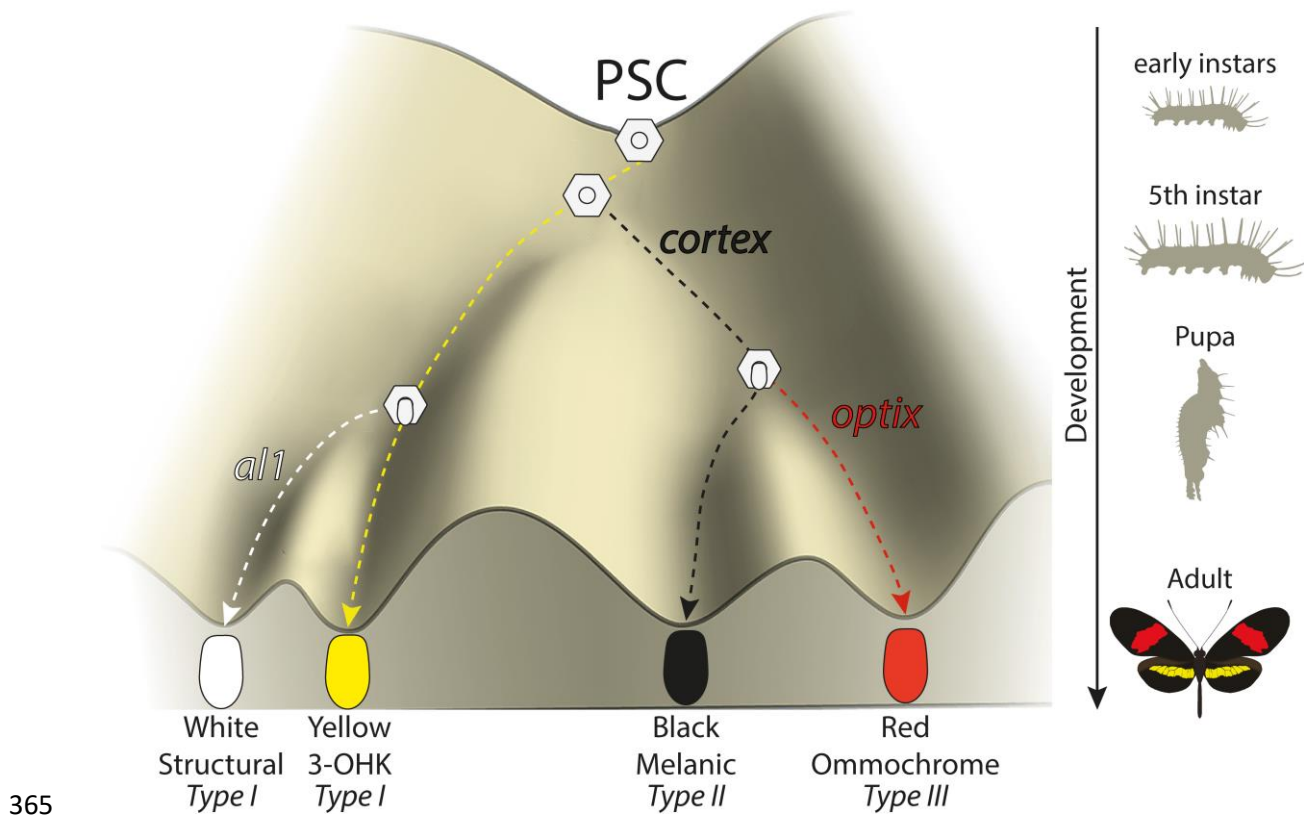


**Figure 8 – Expression of key genes affect scale fate decisions and influence downstream pigmentation state**

During early instar development, wing disc cells differentiate into presumptive scale cells (PSCs). Throughout 5<sup>th</sup> instar growth, PSCs express key scale cell specification genes such as *cortex*, which induce differentiation into Type II (*optix* -) scales or Type III (*optix* +) scales. In the absence of *cortex*, scale cells differentiate into Type I scales which differ in pigmentation state based on 3-OHK synthesis controlled by *aristales1* expression. Model based on the epigenetic landscape (Waddington).

366 However, the switch induced by Cortex under this model is likely not a simple binary toggle, and is  
 367 perhaps dependent on a given protein threshold or heterochrony in expression rather than  
 368 presence/absence, as we find that Cortex protein also localises to the presumptive yellow bar in  
 369 developing pupal wings. Moreover, the *RNA-seq* data presented suggests other linked genes may also  
 370 be playing a role in controlling pattern switches between *Heliconius* races. In particular, we report the  
 371 presence of a bi-cistronic transcript containing the ORFs of the genes *dome* and *wash*, which are  
 372 differentially expressed during early pupal wing development. While a precise role for *dome/wash* in  
 373 wing patterning remains to be demonstrated, it raises the possibility that multiple linked genes co-  
 374 operate during *Heliconius* wing development to drive pattern diversity. It is noteworthy that in the  
 375 locally polymorphic *H. numata*, all wing pattern variation is controlled by inversions surrounding *cortex*

376 and *dome/wash*, both of which are also differentially expressed in *H. numata* (Saenko et al., 2019). This  
377 raises the interesting possibility that evolution has favoured the interaction of multiple genes at the locus  
378 that have since become locked into a supergene in *H. numata*.

### 379 **Conclusions:**

380 The utilization of ‘hotspots’ in evolution has become a recurring theme of evolutionary biology, with  
381 several examples in which independent mutations surrounding the same gene have driven adaptive  
382 evolution (e.g *Pitx1*, *Scute*) (Stern and Orgogozo, 2009). One proposed facilitator of such hotspots is  
383 through the action of genes acting as “input-output” modules, whereby complex spatio-temporal  
384 information is translated into a co-ordinated cell differentiation program, in a simple switch like manner.  
385 One prediction of the nature of such genes would be a switch-like behaviour such as that observed for  
386 *cortex* in this study, as well as the presence of a complex modular *cis*-regulatory architecture  
387 surrounding the gene that is able to integrate the complex upstream positional information into the  
388 switch-like output. A conserved feature of the *cortex* locus in Lepidoptera is the presence of large  
389 intergenic regions surrounding the gene, with evidence these may be acting as modular *cis*-regulatory  
390 switches in *Heliconius* (Enciso-Romero et al., 2017; Van Belleghem et al., 2017), fitting the predicted  
391 structure of input-output genes. Unlike canonical input-output loci however, *cortex* expression appears  
392 not to be restricted to any particular colour pattern element in any given species/race, and yet is capable  
393 of producing a switch-like output (Type I vs Type II/III scales).

394 The genetic locus containing the gene *cortex* has now been implicated in driving wing patterning  
395 differences in many divergent Lepidoptera, and represents one of the more striking cases of parallel  
396 evolution to date. We have shown that it is spatially regulated during larval development, and yet shows  
397 wing-wide cell fate phenotypes leading to a switch in scale cell fate. The amenability of *cortex* to  
398 evolutionary change suggests it may be occupying an unusual position in the GRN underlying scale cell  
399 identity, and may be acting as an input/output gene (Stern and Orgogozo, 2009) that integrates upstream  
400 positional information into a simple on-off switch for scale differentiation. However, it is still unclear  
401 how *cortex* mechanistically affects pigmentation differences, and given its widespread usage throughout  
402 Lepidoptera, it is of general interest to understand its role in driving scale pigmentation.

403

## 404 **Materials and Methods**

### 405 **Butterfly husbandry**

406 *Heliconius* butterflies were collected in the tropical forests of Panama and Ecuador. Adults were  
407 provided with an artificial diet of pollen/glucose solution supplemented with flowers of *Psiguria*,  
408 *Lantana* and/or *Psychotria alata* according to availability. Females were provided with *Passiflora* plants  
409 for egg laying (*P. menispermifolia* for *H. melpomene*, *P. biflora* for *H. erato* and *H. charithonia*, and  
410 *P. vitifolia* for *H. hecale*). Eggs were collected daily, and caterpillars reared on fresh shoots of *P.*  
411 *williamsi* (*melpomene*), *P. biflora* (*erato* and *charithonia*) and *P. vitifolia* for *H. hecale*. Late 5th (final)  
412 instar, caterpillars were separated into individual pots in a temperature-monitored room for *RNA-seq*  
413 experiments, where they were closely observed for the purpose of accurate developmental staging.

### 414 **Phylogenetic analysis of *domeless* and *cortex***

415 To identify orthologs of *dome* across the Lepidoptera we performed tBLASTn searches using the  
416 previously annotated *H. melpomene* Hmel2 (Hm) and *H. erato demophoon* V1 (Hed) *dome* sequences  
417 against the genomes of *Operophtera brumata* V1 (Ob), *Trichoplusia ni* Hi5.VO2 (Tn), *Bombyx mori*  
418 ASM15162v1 (Bm), *Manduca sexta* 1.0 (Ms), *Plodia interpunctella* V1 (Pi), *Amyeolis transitella* V1  
419 (At), *Phoebis sennae* V1.1 (Ps), *Bicyclus anynana* V1.2 (Ba), *Danaus plexippus* V3 (Dp), *Dryas iulia*  
420 helico3 (Di), *Agraulis vanillae* helico3 (Av), *Heliconius erato lativitta* V1 (Hel) genomes found on  
421 Lepbase (Challis et al., 2016). As a trichopteran outgroup we used a recently published Pacbio assembly  
422 of *Stenopsyche tienmushanensis* (St) (Luo et al., 2018). Recovered amino acid translations were aligned  
423 using clustal omega (F. et al., 2019). The resulting alignments were used to produce a phylogenetic tree  
424 using PhyML (Guindon et al., 2010), based on a best fit model using AIC criterion (selected model was  
425 JTT + G + I + F). The tree was visualised and re-rooted to the Trichopteran outgroup using FigTree.

426 To confirm *cortex* as a *cdc20* gene, we retrieved full-length protein homologs from TBLASTN searches  
427 and used them to generate a curated alignment with MAFFT/Guidance2 with a column threshold of 0.5.  
428 We then constructed a maximum-likelihood tree using W-IQ-TREE with the “Auto” function to find a  
429 best-fit model of substitution.

### 430 **Tissue sampling and *RNA-Seq***

431 *H. melpomene rosina* and *H. erato demophoon* butterflies were collected around Gamboa, Panama; *H.*  
432 *melpomene melpomene* and *H. erato hydara* butterflies were collected around Puerto Lara, Darien,  
433 Panama. Methodology for sample preparation and sequencing was performed as previously described  
434 (Hanly et al., 2019). The datasets generated and/or analysed during the current study are available in  
435 the SRA repository (PRJNA552081). Reads from each species were aligned to the respective genome  
436 assemblies Hmel2 (Davey et al., 2016) and Herato\_demophoon\_v1 (Van Belleghem et al., 2017),

437 available on using Hisat2 with default parameters (Kim et al., 2019). The genomes and annotations used  
438 are publicly available at [www.lepbase.org](http://www.lepbase.org). Reads were counted with HTSeq-count in union mode  
439 (Anders et al., 2015) and statistical analysis performed with the R package DESeq2 (Love et al., 2014),  
440 using the GLMI;

441 ~ individual + compartment\*race

442 (Compartments: Anterior Hindwing (HA), Posterior Hindwing (HPo)). *H. melpomene* and *H. erato*  
443 were analysed separately; homology between genes was determined by reciprocal BLAST. Contrasts  
444 were then extracted for comparison of race, compartment, and race given the effect of compartment,  
445 alternating the race used as the base level.

#### 446 ***In situ* hybridizations**

447 Fifth instar larval wing disks and whole mount *in situ* hybridizations were performed following a  
448 published procedure (Martin and Reed, 2014) and imaged using a Leica S4E microscope (Leica  
449 Microsystems). Riboprobe synthesis was performed using the following primers from a 5<sup>th</sup> instar wing  
450 disc cDNA library extracted from *H. melpomene*:

451 Forward primer 5' – CCCGAGATTCTTTCAGCGAAAC -3' and Reverse primer 5' –  
452 ACCGCTCCAACACCAAGAAG – 3'. Templates for riboprobes were designed by attaching a T7  
453 promoter through PCR and performing a DIG labelled transcription reaction (Roche). The same *H.*  
454 *melpomene* probe was used in all *in situ* hybridisation experiments. The resulting probe spanned from  
455 Exon 2 to Exon 7 and was 841bp long.

#### 456 **Immunohistochemistry and image analysis**

457 Pupal wings were dissected around 60 to 70 h post pupation in PBS and fixed at room temperature with  
458 fix buffer (400 µl 4% paraformaldehyde, 600 µl PBS 2mM EGTA) for 30 min. Subsequent washes  
459 were done in wash buffer (0.1% Triton-X 100 in PBS) before blocking the wings at 4°C in block buffer  
460 (0.05 g Bovine Serum Albumin, 10 ml PBS 0.1% Triton-X 100). Wings were then incubated in primary  
461 antibodies against Cortex (1:200, monoclonal rabbit anti-Cortex) at 4°C overnight, washed and added  
462 in secondary antibody (1:500, donkey anti-rabbit IgG, AlexaFlour 555, ThermoFisher Scientific A-  
463 31572). Before mounting, wings were incubated in DAPI with 50% glycerol overnight and finally  
464 transferred to mounting medium (60% glycerol/ 40% PBS 2mM EGTA) for imaging.

465 Z-stacked 2-channelled confocal images were acquired using a Zeiss Cell Observer Spinning Disk  
466 Confocal microscope. Image processing was done using FIJI plugins Trainable Weka Segmentation  
467 and BioVoxxel (Arganda-Carreras et al., 2017; Brocher, Jan, 2014; Schindelin et al., 2012). Manual  
468 tracing of nuclei was input for machine learning and processing of images to obtain final thresholded  
469 images, then an overlay of Cortex puncta with DAPI nuclei staining identified regions of nuclei

470 containing Cortex puncta. Spatial analysis of image data was conducted using R software 4.0.0 package  
471 Spatstat (Baddeley and Turner, 2005).

#### 472 **CRISPR/Cas9 genome editing**

473 Guide RNAs were designed corresponding to GGN<sub>20</sub>NGG sites located within the *cortex* coding region  
474 using the program Geneious (Kearse et al., 2012). To increase target specificity, guides were checked  
475 against an alignment of both *melpomene* and *erato* re-sequence data at the scaffolds containing the  
476 *cortex* gene (Moest et al., 2020; Van Belleghem et al., 2017), and selected based on sequence  
477 conservation across populations. Based on these criteria, each individual guide was checked against the  
478 corresponding genome for off-target effects, using the default Geneious algorithm. Guide RNAs with  
479 high conservation and low off-target scores were then synthesised following the protocol by Bassett  
480 and Liu, 2014. Injections were performed following procedures described in Mazo-Vargas et al., 2017,  
481 within 1-4 hours of egg laying. Several combinations of guide RNAs for separate exons at different  
482 concentrations were used for different injection experiments (Supplementary File 7). For *H. charithonia*  
483 we used the *H. erato* specific guides and for *H. hecale* we used the *H. melpomene* guides.

#### 484 **Genotyping**

485 DNA was extracted from mutant leg tissue and amplified using oligonucleotides flanking the sgRNAs  
486 target region (Supplementary File 6). PCR amplicons were column purified, subcloned into the pGEM-  
487 T Easy Vector System (Promega) and sequenced on an ABI 3730 sequencer.

#### 488 **Scanning Electron Microscopy (SEM) Imaging**

489 Individual scales from wild type and mutant regions of interest were collected by brushing the surface  
490 of the wing with an eyelash tool, then dusted onto an SEM stub with double-sided carbon tape. Stubs  
491 were then colour imaged under the Keyence VHX-5000 microscope for registration of scale type.  
492 Samples were sputter-coated with one 12.5 nm layer of gold for improving sample conductivity. SEM  
493 images were acquired on a FEI Teneo LV SEM, using secondary electrons (SE) and an Everhart-  
494 Thornley detector (ETD) using a beam energy of 2.00 kV, beam current of 25 pA, and a 10 µs dwell  
495 time. Individual images were stitched using the Maps 3.10 software (ThermoFisher Scientific).

#### 496 **Morphometrics analysis**

497 Morphometric measurements of scale widths and ridge distances were carried out on between 10 and  
498 20 scales of each type, using a custom semi-automated R pipeline that derives ultrastructural  
499 parameters from large SEM images (Day et al., 2019). Briefly, ridge spacing was assessed by Fourier  
500 transforming intensity traces of the ridges acquired from the FIJI software (Schindelin et al.,  
501 2012). Scale width was directly measured in FIJI by manually tracing a line, orthogonal to the ridges,  
502 at the section of maximal width.

## 503 **Author Contributions**

504 C.D.J., L.L., J.J.H., A.M., and W.O.M. designed the research; L.L., J.J.H., L.S.L., A.R., I.A.W.,  
505 C.C., C.W., J.M.W., J.F., H.A.C., L.R.B. performed research. L.L wrote the paper. C.D.J and  
506 W.O.M contributed equally.

## 507 **Acknowledgements**

508 We thank Oscar Paneso, Elizabeth Evans, Rachel Crisp and Cruz Batista, for technical support with  
509 rearing of butterflies and CRISPR larvae, and to Markus Möest, Steven Van Belleghem and Tim  
510 Thurman for assistance with butterfly collection. We are also grateful to Krzysztof “Chris” Kozak and  
511 Chi Yun for thoughtful discussions and feedback on the manuscript. We thank the GW Nanofabrication  
512 and Imaging Center forenabling SEM, and in particular Christine Brantner and Anastas Popratiloff for  
513 their technical assistance

## 514 **Competing interests**

515 The authors declare no competing interests.

516

## 517 **References**

- 518 Anders S, Pyl PT, Huber W. 2015. HTSeq--a Python framework to work with high-throughput  
519 sequencing data. *Bioinformatics* **31**:166–169. doi:10.1093/bioinformatics/btu638
- 520 Arganda-Carreras I, Kaynig V, Rueden C, Eliceiri KW, Schindelin J, Cardona A, Sebastian Seung H.  
521 2017. Trainable Weka Segmentation: a machine learning tool for microscopy pixel  
522 classification. *Bioinformatics* **33**:2424–2426. doi:10.1093/bioinformatics/btx180
- 523 Aymone ACB, Valente VLS, de Araújo AM. 2013. Ultrastructure and morphogenesis of the wing  
524 scales in *Heliconius erato phyllis* (Lepidoptera: Nymphalidae): What silvery/brownish  
525 surfaces can tell us about the development of color patterning? *Arthropod Structure &*  
526 *Development* **42**:349–359. doi:10.1016/j.asd.2013.06.001
- 527 Baddeley A, Turner R. 2005. spatstat: An R Package for Analyzing Spatial Point Patterns. *Journal of*  
528 *Statistical Software* **12**:1–42. doi:10.18637/jss.v012.i06
- 529 Bassett A, Liu J-L. 2014. CRISPR/Cas9 mediated genome engineering in *Drosophila*. *Methods* **69**:128–  
530 136. doi:10.1016/j.ymeth.2014.02.019
- 531 Beldade P, Saenko SV, Pul N, Long AD. 2009. A Gene-Based Linkage Map for *Bicyclus anynana*  
532 Butterflies Allows for a Comprehensive Analysis of Synteny with the Lepidopteran Reference  
533 Genome. *PLOS Genetics* **5**:e1000366. doi:10.1371/journal.pgen.1000366



- 534 Brocher, Jan. 2014. Qualitative and Quantitative Evaluation of Two New Histogram Limiting  
535 Binarization Algorithms. *Computer Science Journals* **8**:30–48.
- 536 Brown KS. 1981. The Biology of Heliconius and Related Genera. *Annual Review of Entomology*  
537 **26**:427–457. doi:10.1146/annurev.en.26.010181.002235
- 538 Challi RJ, Kumar S, Dasmahapatra KK, Jiggins CD, Blaxter M. 2016. Lepbase: the Lepidopteran  
539 genome database. *bioRxiv* 056994. doi:10.1101/056994
- 540 Cho EH, Nijhout HF. 2013. Development of polyploidy of scale-building cells in the wings of *Manduca*  
541 *sexta*. *Arthropod Struct Dev* **42**:37–46. doi:10.1016/j.asd.2012.09.003
- 542 Chu T, Henrion G, Haegeli V, Strickland S. 2001. Cortex, a *Drosophila* gene required to complete  
543 oocyte meiosis, is a member of the Cdc20/fizzy protein family. *Genesis* **29**:141–152.  
544 doi:10.1002/gene.1017
- 545 Concha C, Wallbank RWR, Hanly JJ, Fenner J, Livraghi L, Rivera ES, Paulo DF, Arias C, Vargas M,  
546 Sanjeev M, Morrison C, Tian D, Aguirre P, Ferrara S, Foley J, Pardo-Diaz C, Salazar C, Linares  
547 M, Massardo D, Counterman BA, Scott MJ, Jiggins CD, Papa R, Martin A, McMillan WO. 2019.  
548 Interplay between Developmental Flexibility and Determinism in the Evolution of Mimetic  
549 Heliconius Wing Patterns. *Current Biology* S0960982219313168.  
550 doi:10.1016/j.cub.2019.10.010
- 551 Courtier-Orgogozo V, Arnoult L, Prigent SR, Wiltgen S, Martin A. 2020. Gephebase, a database of  
552 genotype–phenotype relationships for natural and domesticated variation in Eukaryotes.  
553 *Nucleic Acids Res* **48**:D696–D703. doi:10.1093/nar/gkz796
- 554 Davey JW, Chouteau M, Barker SL, Maroja L, Baxter SW, Simpson F, Merrill RM, Joron M, Mallet J,  
555 Dasmahapatra KK, Jiggins CD. 2016. Major Improvements to the Heliconius melpomene  
556 Genome Assembly Used to Confirm 10 Chromosome Fusion Events in 6 Million Years of  
557 Butterfly Evolution. *G3: Genes, Genomes, Genetics* **6**:695–708. doi:10.1534/g3.115.023655
- 558 Day CR, Hanly JJ, Ren A, Martin A. 2019. Sub-micrometer insights into the cytoskeletal dynamics and  
559 ultrastructural diversity of butterfly wing scales. *Dev Dyn* **248**:657–670. doi:10.1002/dvdy.63
- 560 Enciso-Romero J, Pardo-Díaz C, Martin SH, Arias CF, Linares M, McMillan WO, Jiggins CD, Salazar C.  
561 2017. Evolution of novel mimicry rings facilitated by adaptive introgression in tropical  
562 butterflies. *Molecular Ecology* **26**:5160–5172. doi:10.1111/mec.14277
- 563 F M, Ym P, J L, N B, T G, N M, P B, Arn T, Sc P, Rd F, R L. 2019. The EMBL-EBI search and sequence  
564 analysis tools APIs in 2019. *Nucleic Acids Res* **47**:W636–W641. doi:10.1093/nar/gkz268
- 565 Finkbeiner SD, Fishman DA, Osorio D, Briscoe AD. 2017. Ultraviolet and yellow reflectance but not  
566 fluorescence is important for visual discrimination of conspecifics by *Heliconius erato*.  
567 *Journal of Experimental Biology* **220**:1267–1276. doi:10.1242/jeb.153593

- 568 Gilbert LE, Forrest HS, Schultz TD, Harvey DJ. 1987. Correlations of ultrastructure and pigmentation  
569 suggest how genes control development of wing scales of *Heliconius* butterflies. *The Journal*  
570 *of research on the Lepidoptera (USA)*.
- 571 Greenstein ME. 1972. The ultrastructure of developing wings in the giant silkmoth, *Hyalophora*  
572 *cecropia*. II. Scale-forming and socket-forming cells. *J Morphol* **136**:23–51.  
573 doi:10.1002/jmor.1051360103
- 574 Guindon S, Dufayard J-F, Lefort V, Anisimova M, Hordijk W, Gascuel O. 2010. New Algorithms and  
575 Methods to Estimate Maximum-Likelihood Phylogenies: Assessing the Performance of  
576 PhyML 3.0. *Systematic Biology* **59**:307–321. doi:10.1093/sysbio/syq010
- 577 Hanly JJ, Wallbank RWR, McMillan WO, Jiggins CD. 2019. Conservation and flexibility in the gene  
578 regulatory landscape of heliconiine butterfly wings. *EvoDevo* **10**:15. doi:10.1186/s13227-  
579 019-0127-4
- 580 Henke K, Pohley H-J. 1952. Differentielle Zellteilungen und Polyploidie bei der Schuppenbildung der  
581 Mehlmotte *Ephestia kühniella* Z. *Zeitschrift für Naturforschung B* **7**:65–79. doi:10.1515/znb-  
582 1952-0201
- 583 Huber B, Whibley A, Poul YL, Navarro N, Martin A, Baxter S, Shah A, Gilles B, Wirth T, McMillan WO,  
584 Joron M. 2015. Conservatism and novelty in the genetic architecture of adaptation in  
585 *Heliconius* butterflies. *Heredity* **114**:515–524. doi:10.1038/hdy.2015.22
- 586 Ito K, Katsuma S, Kuwazaki S, Jouraku A, Fujimoto T, Sahara K, Yasukochi Y, Yamamoto K, Tabunoki H,  
587 Yokoyama T, Kadono-Okuda K, Shimada T. 2016. Mapping and recombination analysis of two  
588 moth colour mutations, Black moth and Wild wing spot, in the silkworm *Bombyx mori*.  
589 *Heredity* **116**:52–59. doi:10.1038/hdy.2015.69
- 590 Iwata M, Otaki JM. 2016. Spatial patterns of correlated scale size and scale color in relation to color  
591 pattern elements in butterfly wings. *Journal of Insect Physiology* **85**:32–45.  
592 doi:10.1016/j.jinsphys.2015.11.013
- 593 Jiggins CD. 2017. *The Ecology and Evolution of Heliconius Butterflies*. Oxford University Press.
- 594 Jiggins CD, McMillan WO. 1997. The genetic basis of an adaptive radiation: warning colour in two  
595 *Heliconius* species. *Proc Biol Sci* **264**:1167–1175. doi:10.1098/rspb.1997.0161
- 596 Joron M, Papa R, Beltrán M, Chamberlain N, Mavárez J, Baxter S, Abanto M, Bermingham E,  
597 Humphray SJ, Rogers J, Beasley H, Barlow K, H. ffrench-Constant R, Mallet J, McMillan WO,  
598 Jiggins CD. 2006. A Conserved Supergene Locus Controls Colour Pattern Diversity in  
599 *Heliconius* Butterflies. *PLoS Biol* **4**:e303. doi:10.1371/journal.pbio.0040303
- 600 Kearse M, Moir R, Wilson A, Stones-Havas S, Cheung M, Sturrock S, Buxton S, Cooper A, Markowitz S,  
601 Duran C, Thierer T, Ashton B, Meintjes P, Drummond A. 2012. Geneious Basic: an integrated

- 602 and extendable desktop software platform for the organization and analysis of sequence  
603 data. *Bioinformatics* **28**:1647–1649. doi:10.1093/bioinformatics/bts199
- 604 Kim D, Paggi JM, Park C, Bennett C, Salzberg SL. 2019. Graph-based genome alignment and  
605 genotyping with HISAT2 and HISAT-genotype. *Nat Biotechnol* **37**:907–915.  
606 doi:10.1038/s41587-019-0201-4
- 607 Koch PB. 1993. Production of [14C]-Labeled 3-Hydroxy-L-Kynurenine in a Butterfly, *Heliconius*  
608 *charitonia* L. (Heliconidae), and Precursor Studies in Butterfly Wing Ommatins. *Pigment Cell*  
609 *Research* **6**:85–90. doi:10.1111/j.1600-0749.1993.tb00586.x
- 610 Kronforst MR, Papa R. 2015. The Functional Basis of Wing Patterning in *Heliconius* Butterflies: The  
611 Molecules Behind Mimicry. *Genetics* **200**:1–19. doi:10.1534/genetics.114.172387
- 612 Lamas G, editor. 2004. Atlas Of Neotropical Lepidoptera: Checklist Pt. 4a Hesperioidea-papilionoidea.  
613 Gainesville: Scientific Pub.
- 614 Lewis JJ, Geltman RC, Pollak PC, Rondem KE, Belleghem SMV, Hubisz MJ, Munn PR, Zhang L, Benson  
615 C, Mazo-Vargas A, Danko CG, Counterman BA, Papa R, Reed RD. 2019. Parallel evolution of  
616 ancient, pleiotropic enhancers underlies butterfly wing pattern mimicry. *PNAS* **116**:24174–  
617 24183. doi:10.1073/pnas.1907068116
- 618 Love MI, Huber W, Anders S. 2014. Moderated estimation of fold change and dispersion for RNA-seq  
619 data with DESeq2. *Genome Biol* **15**:550. doi:10.1186/s13059-014-0550-8
- 620 Luo S, Tang M, Frandsen PB, Stewart RJ, Zhou X. 2018. The genome of an underwater architect, the  
621 caddisfly *Stenopsyche tienmushanensis* Hwang (Insecta: Trichoptera). *Gigascience* **7**.  
622 doi:10.1093/gigascience/giy143
- 623 Martin A, Courtier-Orgogozo V. 2017. Morphological Evolution Repeatedly Caused by Mutations in  
624 Signaling Ligand Genes In: Sekimura T, Nijhout HF, editors. Diversity and Evolution of  
625 Butterfly Wing Patterns: An Integrative Approach. Singapore: Springer. pp. 59–87.  
626 doi:10.1007/978-981-10-4956-9\_4
- 627 Martin A, Papa R, Nadeau NJ, Hill RI, Counterman BA, Halder G, Jiggins CD, Kronforst MR, Long AD,  
628 McMillan WO, Reed RD. 2012. Diversification of complex butterfly wing patterns by  
629 repeated regulatory evolution of a Wnt ligand. *Proc Natl Acad Sci USA* **109**:12632–12637.  
630 doi:10.1073/pnas.1204800109
- 631 Martin A, Reed RD. 2014. Wnt signaling underlies evolution and development of the butterfly wing  
632 pattern symmetry systems. *Developmental Biology* **395**:367–378.  
633 doi:10.1016/j.ydbio.2014.08.031
- 634 Matsuoka Y, Monteiro A. 2018. Melanin Pathway Genes Regulate Color and Morphology of Butterfly  
635 Wing Scales. *Cell Reports* **24**:56–65. doi:10.1016/j.celrep.2018.05.092

- 636 Mazo-Vargas A, Concha C, Livraghi L, Massardo D, Wallbank RWR, Zhang L, Papador JD, Martinez-  
637 Najera D, Jiggins CD, Kronforst MR, Breuker CJ, Reed RD, Patel NH, McMillan WO, Martin A.  
638 2017. Macroevolutionary shifts of WntA function potentiate butterfly wing-pattern diversity.  
639 *PNAS* **114**:10701–10706. doi:10.1073/pnas.1708149114
- 640 Moest M, Belleghem SMV, James JE, Salazar C, Martin SH, Barker SL, Moreira GRP, Mérot C, Joron M,  
641 Nadeau NJ, Steiner FM, Jiggins CD. 2020. Selective sweeps on novel and introgressed  
642 variation shape mimicry loci in a butterfly adaptive radiation. *PLOS Biology* **18**:e3000597.  
643 doi:10.1371/journal.pbio.3000597
- 644 Nadeau NJ. 2016. Genes controlling mimetic colour pattern variation in butterflies. *Current Opinion*  
645 *in Insect Science, Global change biology \* Molecular physiology* **17**:24–31.  
646 doi:10.1016/j.cois.2016.05.013
- 647 Nadeau NJ, Pardo-Diaz C, Whibley A, Supple MA, Saenko SV, Wallbank RWR, Wu GC, Maroja L,  
648 Ferguson L, Hanly JJ, Hines H, Salazar C, Merrill RM, Dowling AJ, ffrench-Constant RH,  
649 Llaurens V, Joron M, McMillan WO, Jiggins CD. 2016. The gene cortex controls mimicry and  
650 crypsis in butterflies and moths. *Nature* **534**:106–110. doi:10.1038/nature17961
- 651 Pesin JA, Orr-Weaver TL. 2007. Developmental Role and Regulation of cortex, a Meiosis-Specific  
652 Anaphase-Promoting Complex/Cyclosome Activator. *PLOS Genetics* **3**:e202.  
653 doi:10.1371/journal.pgen.0030202
- 654 Prud'homme B, Gompel N, Carroll SB. 2007. Emerging principles of regulatory evolution. *PNAS*  
655 **104**:8605–8612. doi:10.1073/pnas.0700488104
- 656 Raff JW, Jeffers K, Huang J. 2002. The roles of Fzy/Cdc20 and Fzr/Cdh1 in regulating the destruction  
657 of cyclin B in space and time. *J Cell Biol* **157**:1139–1149. doi:10.1083/jcb.200203035
- 658 Reed RD, McMillan WO, Nagy LM. 2008. Gene expression underlying adaptive variation in *Heliconius*  
659 wing patterns: non-modular regulation of overlapping cinnabar and vermilion prepatterns.  
660 *Proc Biol Sci* **275**:37–46. doi:10.1098/rspb.2007.1115
- 661 Reed RD, Papa R, Martin A, Hines HM, Counterman BA, Pardo-Diaz C, Jiggins CD, Chamberlain NL,  
662 Kronforst MR, Chen R, Halder G, Nijhout HF, McMillan WO. 2011. optix drives the repeated  
663 convergent evolution of butterfly wing pattern mimicry. *Science* **333**:1137–1141.  
664 doi:10.1126/science.1208227
- 665 Rosser N, Phillimore AB, Huertas B, Willmott KR, Mallet J. 2012. Testing historical explanations for  
666 gradients in species richness in heliconiine butterflies of tropical America: DIVERSIFICATION  
667 OF BUTTERFLIES. *Biological Journal of the Linnean Society* **105**:479–497. doi:10.1111/j.1095-  
668 8312.2011.01814.x

- 669 Saenko SV, Chouteau M, Piron-Prunier F, Blugeon C, Joron M, Llaurens V. 2019. Unravelling the  
670 genes forming the wing pattern supergene in the polymorphic butterfly *Heliconius numata*.  
671 *Evodevo* **10**:16. doi:10.1186/s13227-019-0129-2
- 672 Schaeffer V, Althausen C, Shcherbata HR, Deng W-M, Ruohola-Baker H. 2004. Notch-Dependent  
673 Fizzy-Related/Hec1/Cdh1 Expression Is Required for the Mitotic-to-Endocycle Transition in  
674 *Drosophila* Follicle Cells. *Current Biology* **14**:630–636. doi:10.1016/j.cub.2004.03.040
- 675 Schindelin J, Arganda-Carreras I, Frise E, Kaynig V, Longair M, Pietzsch T, Preibisch S, Rueden C,  
676 Saalfeld S, Schmid B, Tinevez J-Y, White DJ, Hartenstein V, Eliceiri K, Tomancak P, Cardona A.  
677 2012. Fiji: an open-source platform for biological-image analysis. *Nat Methods* **9**:676–682.  
678 doi:10.1038/nmeth.2019
- 679 Shcherbata HR. 2004. The mitotic-to-endocycle switch in *Drosophila* follicle cells is executed by  
680 Notch-dependent regulation of G1/S, G2/M and M/G1 cell-cycle transitions. *Development*  
681 **131**:3169–3181. doi:10.1242/dev.01172
- 682 Stern DL, Orgogozo V. 2009. Is Genetic Evolution Predictable? *Science* **323**:746–751.  
683 doi:10.1126/science.1158997
- 684 Swan A, Schüpbach T. 2007. The Cdc20 (Fzy)/Cdh1-related protein, Cort, cooperates with Fzy in  
685 cyclin destruction and anaphase progression in meiosis I and II in *Drosophila*. *Development*  
686 **134**:891–899. doi:10.1242/dev.02784
- 687 Thayer RC, Allen FI, Patel NH. 2020. Structural color in *Junonia* butterflies evolves by tuning scale  
688 lamina thickness. *eLife* **9**:e52187. doi:10.7554/eLife.52187
- 689 Turner JRG. 1981. Adaptation and Evolution in *Heliconius*: A Defense of NeoDarwinism. *Annual*  
690 *Review of Ecology and Systematics* **12**:99–121. doi:10.1146/annurev.es.12.110181.000531
- 691 Van Belleghem SM, Rastas P, Papanicolaou A, Martin SH, Arias CF, Supple MA, Hanly JJ, Mallet J,  
692 Lewis JJ, Hines HM, Ruiz M, Salazar C, Linares M, Moreira GRP, Jiggins CD, Counterman BA,  
693 McMillan WO, Papa R. 2017. Complex modular architecture around a simple toolkit of wing  
694 pattern genes. *Nature Ecology & Evolution* **1**:1–12. doi:10.1038/s41559-016-0052
- 695 VanKuren NW, Massardo D, Nallu S, Kronforst MR. 2019. Butterfly mimicry polymorphisms highlight  
696 phylogenetic limits of gene re-use in the evolution of diverse adaptations. *Mol Biol Evol.*  
697 doi:10.1093/molbev/msz194
- 698 Van't Hof AE, Campagne P, Rigden DJ, Yung CJ, Lingley J, Quail MA, Hall N, Darby AC, Saccheri IJ.  
699 2016. The industrial melanism mutation in British peppered moths is a transposable  
700 element. *Nature* **534**:102–105. doi:10.1038/nature17951

- 701 van't Hof AE, Reynolds LA, Yung CJ, Cook LM, Saccheri IJ. 2019. Genetic convergence of industrial  
702 melanism in three geometrid moths. *Biology Letters* **15**:20190582.  
703 doi:10.1098/rsbl.2019.0582
- 704 Westerman EL, VanKuren NW, Massardo D, Tenger-Trolander A, Zhang W, Hill RI, Perry M, Bayala E,  
705 Barr K, Chamberlain N, Douglas TE, Buerkle N, Palmer SE, Kronforst MR. 2018. Aristaless  
706 Controls Butterfly Wing Color Variation Used in Mimicry and Mate Choice. *Curr Biol* **28**:3469-  
707 3474.e4. doi:10.1016/j.cub.2018.08.051
- 708 Zhang L, Mazo-Vargas A, Reed RD. 2017. Single master regulatory gene coordinates the evolution  
709 and development of butterfly color and iridescence. *PNAS* **114**:10707–10712.  
710 doi:10.1073/pnas.1709058114